Int. J. Environ. Res., 5(4):939-950, Autumn 2011
ISSN: 1735-6865

Modeling Seasonal Rainfall Erosivity on a Regional scale: A case Study from Northeastern Iran

Kavian, A.*, Fathollah Nejad, Y. , Habibnejad, M. and Soleimani, K.

Department of Rangeland & Watershed Management Engineering, Sari Agricultural Sciences and Natural Resources University, Sari, Iran

Received 29 Sep. 2010; Revised 4 March 2011; Accepted 17 March 2011

ABSTRACT: There is a need to analyze and map rainfall erosivity to assess soil erosion at the regional scale. The objectives of this study were to develop a regional model to estimate seasonal erosivity from seasonal rainfall data and to study temporal and spatial distribution of rainfall erosivity for the Gorganrood drainage basin in the northeast of Iran. Six gauging stations with a high temporal resolution (15 min) and eleven monthly totals stations located into the study area have been used. Regression models for pluviograph stations indicated that storm rainfall explained 22–51% of the variation in storm erosivity. But, at the seasonal scale, the explained variation increased to 62–86% and modified coefficient of efficiency increased from 0.12-0.29 to 0.38-0.64. Also, the results of ANOVA showed that EI_{30} values have significant difference between autumn/ summer seasons and winter/spring seasons. Interpolation surfaces were created from all 17 stations seasonal values using the local polynomial algorithm. The results showed, during the wet season, erosivity varied from 438 Mj/mm/h (west) to 1015 Mj/ mm/h (Middle). But, in the dry season, values of erosivity were lower than from values in wet season and the highest values were at the middle parts of the study area and the lowest were at the eastern and the western parts of the study area. Our findings provide good guidance to integrate pluviograph and pluviometric data for rainfall erosivity assessment in regional scales, where short duration rainfall intensity data, usually are not available.

Key words: Soil erosion, Spatial variability, Local Polynomial Algorithm, Gorganrood Drainage Basin

INTRODUCTION

It is well known that a few, very intense rainfall events are responsible for the largest part of the soil erosion (Gonzalez-Hidalgo *et al.,* 2007). Among the natural factors affecting soil erosion, rainfall erosivity has a paramount importance. Rainfall erosivity is defined as the aggressiveness of the rain to cause erosion (Lal, 1990).

The Universal Soil Loss Equation (USLE) (Wischmeier and Smith, 1978) and its revised forms (RUSLE) (Renard *et al.,* 1997; Foster, 2004) are the most frequently applied worldwide for predicting the annual soil loss based on rainfall erosivity, topography and land-use (Abu Hammad *et al.,* 2004). However, properly application of these models to provide annual soil loss depends on knowledge of hourly or sub-hourly distribution of rainfall intensities. Rainfall erosivity can be quantified by several erosivity indices which evaluate the relationship between drop size distribution or maximum intensity during a period of time and kinetic energy of given storm (Lal, 1998). From these indices, the EI_{30} (R) index has been the most commonly used in the world. To compute storm EI_{30} values, continuous rainfall intensity data are needed. Short duration rainfall intensity data are obtained today by either digital pluviographs or tipping-bucket technology (discrete rainfall rates) but, for many parts of the world (including the study area) the spatial and temporal coverage of pluviograph data are usually limited (Yu *et al.,* 2001).

In areas where long-term rainfall intensity records were not available, several researchers have used indirect regression techniques to estimate EI_{30} index based on other available data such as daily, monthly and annual records of rainfall depth (Renard and Freimound, 1994; Sadeghi and Behzadfar, 2005). Yu (1998) reported that the relationship between rainfall depth and erosivity is region specific. Mapping rainfall erosivity at regional scale using GIS techniques is still an emerging research question, especially in Iran, because there are not sufficient data about soil erosion and sediment yield as well as validated physically based-distributed soil erosion and sediment yield models. EI_{30} index map allows for a better

*Corresponding author E-mail: a.kavian@sanru.ac.ir

comprehension of soil erosion conservation assessment (Whinchel *et al.,* 2008). Several authors have used local polynomial algorithm and inverse distance weighted (IDW) as GIS techniques to map EI_{30} index by means of interpolation methods (Shi, 2004; Lim, 2005; Mutua, 2006; Men *et al.,* 2008, Angulo-Martýnez *et al.,* 2009).

There are few studies to compare interpolation techniques for rainfall erosivity indices. Millward (1999) calculated the EI30 index at the monthly scale and the R factor with geostatistics and IDW techniques for the Algarve region (Southern Portugal). Hoyos *et al.,* (2005) reported that a local polynomial algorithm gave better results than the IDW in the Colombian Andes. Goovaerts (1999) discussed the relation between rainfall erosivity and elevation in the comparison of three different geostatistical methods. Nonetheless, none of these works created a comprehensive comparison of mapping methods at the regional scale.

MATERIALS & METHODS

The present study has been undertaken for the Gorganrood drainage basin in the northeast of Iran. The basin covers an area of 10197 km^2 and it drains a large area of the Golestan Province between the latitudes 36° 35′ and 38° 15′ N and longitudes 45° 10′ and 56° 26′ E (Fig. 1). Elevations range from -21 to 3945 m with a relief characterized by mean elevation about 907 m and low gradients about 1.27%. The mean annual rainfall in the area is 491 mm with ranges between 252.6 in the west and 641.3 mm in the east. Monthly rainfall amounts are also varying and the area experiences two periods of high rainfall separated by two periods of low rainfall. The primary maximum generally occurs between January-March, while the secondary maximum generally occurs in June-November. The primary minimum occurs in March-June and the secondary minimum generally occurs in November-January. Major land uses in the study area include forest, agriculture and pasture (36, 34 and 18%).

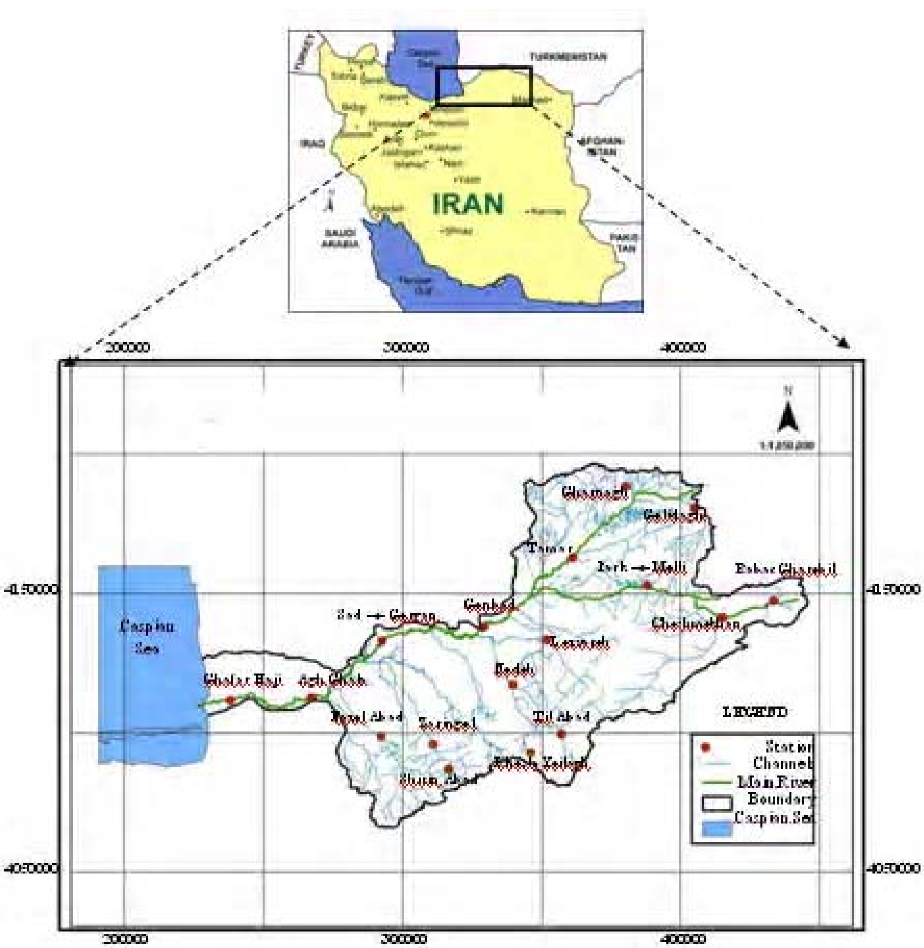

Fig. 1. The upper map shows the situation of Goorganrod Basin in the Iran. The beneath map shows the location of 10197 km^2 Goorganrod Basin. The locations of the meteorological stations are shown by the red circle. The location of the Caspian Sea also shows in the map to the west of Goorganrod Basin

Golestan province in the Northeast of Iran, suffered many floods in years 2001 to 2003. Loss of property in the flood August 2001 was about 50 millions of dollars. In this event 256 persons dead and many people had injury and untraceable and the roads of 180 villages were blocked. Similar floods were happened in years 2002 and 2003. Moreover, much volumes of sediment deliver to 2 dams in the down stream of the flooded area. So, it is necessary to investigate rainfall erosivity in order to better understanding of hydrological processes in the study area.

The data base consisted from six gauging stations located into the study area (Fig. 1). Each station provides precipitation data at a time resolution of 15 minute. A period of 13 years (1 January 1993 to 31 December 2005) was selected to analyze erosivity because it represented a reasonable compromise between the number of available stations and the amount of data to be analyzed. The rainfall data were subjected to a quality control that allowed identifying wrong records. These records were replaced by the corresponding ones from a nearby station. This allowed creating an erosive events data base. The erosive events were determined by the RUSLE criterion (Renard *et al.,* 1997): an event is considered erosive if at least one of this conditions true: 1) the cumulative rainfall is greater than 12.7 mm, or 2) the cumulative rainfall has at least one peak greater than 6.35 mm in 15 min. Two consecutive events are considered different from each other if the cumulative rainfall in a period of 6 hours is greater than 12.7 mm.

In the study area all six gauging stations had imperfect data for a < 1 years. Total daily rainfall was available in this period but intensity data were not available to compute erosivity, directly. So, two following methods were applied to complete records:

1.Days added when daily rainfall was equal to or greater than 12.7 mm based on RUSLE methodology (Renard *et al.,* 1997).

2.A relationship between storm rainfall (independent) and storm EI_{30} (dependent) was developed using regression methods in each stations, separately. Both variables were transformed to log scale and a linear regression was performed for each station. Then, these relationships were applied to complete missing EI_{30} values.

EI30 index have chosen to compute erosivity, because in the literature, the most known and widely used indices to predict the erosive potential of raindrop impact is the EI_{30} (R) index. Individual storm EI_{30} values were computed following the RUSLE methodology (Renard *et al.,* 1997) using erosive events data base from six gauging stations located in the study area. Within each gauging stations, storm EI_{30} values were added on a seasonal basis.

The predicted values of EI_{30} in different time scales were evaluated by coefficient of determination (R^2), the root mean square error (RMSE), coefficient of efficiency (E) and modified coefficient of efficiency (E1) values.

The RMSE (Thomann, 1982) is defined as:

$$RMSE = \sqrt{\frac{\sum_{i=1}^{n}(O_i - P_i)^2}{n}}$$

Where O_i and P_i are the observed and predicted values for the ith pair, and n is the total number of paired values. The smaller the RMSE, the closer the predicted values are to observed values.

The coefficient of efficiency (E) (Nash and Sutcliffe, 1970) is expressed as:

$$E = 1.0 - \frac{\sum_{i=1}^{n}(Oi - Pi)^2}{\sum_{i=1}^{n}(Oi - \bar{O})^2}$$

Where $\bar{O}$ is the mean of observed values and other parameters are defined above. The model efficiency can range from - ∞ to 1, and the closer the values is to 1, the better are the predictions. A value of zero indicates that the observed mean is as good a predictor as the model itself. While the negative value results when there is a greater difference between observed and predicted values than between observed and the mean of observed values (Warner *et al.,* 1997).

Because values are squared, this coefficient is very sensitive to extreme values. So, the modified coefficient of efficiency (E1) is defined as (Legates and McCabe, 1999):

$$E_1 = 1.0 - \frac{\sum_{i=1}^{n}|O_i - P_i|}{\sum_{i=1}^{n}|O_i - \bar{O}|}$$

The seasonal erosivity models from the pluviographic stations were applied to develop a model in regional scale, so that pluviographic rainfall data could be used to predict seasonal erosivity. Model performance was evaluated using the indices already mentioned. Then, analysis of variance (ANOVA) (Julie, 2001) was applied to determine differences among seasonal EI_{30} values for each station.

Also, monthly rainfall data for 11 stations into the study area were available (Fig. 1 and Table. 1). These data were classified into seasons and used with the regional regression model to create seasonal EI_{30} values for each pluviometric station.

Two interpolation methods, inverse distance weighted (IDW) and local polynomial were applied to model and map spatial variability of seasonal erosivity data through ArcGIS geostatistical Analyst (Johnston *et al.,* 2001). The final surface was selected as that one combining the lowest prediction error and being physically meaningful.

RESULTS & DISCUSSION

The intensity data from 420 storms in the period of 12 years were applied to compute the EI_{30} index at six pluviographic stations. The regression analysis was used to model the relationship between storm rain and EI_{30} and to complete the data sets for each station. These models indicated that storm rainfall explained 22–51% of the variation in storm erosivity. The results showed similar adjusted R^2 and E values while the E_1 values are lower than above mentioned criterions (Table 2).

Coefficient of determination of the developed regression models between rain amount and erosivity indicated that, at the storm level, rainfall explained 22 and 51% of the variability in EI_{30}. Model performance was very similar in stations Lezvareh, Park Melli and Golidagh. But in Agh ghala, model performance was lower than other stations.

Analysis of correlation between daily totals and storm rainfall showed coefficient of Pearson's r ranging from 0.93 to 0.96, that indicated daily rainfall was a reliable substitute for storm rainfall during years with missing storm data. So, data sets for each station were accomplished to compute seasonal EI_{30} values by adding storm EI_{30} values in each season. The results showed seasonal EI_{30} values had a similar pattern to rainfall with lower values in the winter and spring seasons and higher values in the autumn and summer season (Table 3). Also, the results of ANOVA verify these results (Table 3). These results showed that EI_{30} values have significant difference between autumn/ summer seasons and winter/spring seasons. In 4 stations (with the exception of Agh Ghala and Ghafarhaji stations), there was no significant difference at the level of 5% between EI_{30} values among autumn and spring seasons. In the Lezvareh station, so, there was no significant difference between four seasons. More results explanation is possible from Table 3. The results of this study showed that coefficient of determination and model performance were increased when seasonal data were applied. Yu and Rosewell, (1996) showed similar results. Model performance at the seasonal time scale was high for all stations. The highest value of model performance was calculated in Lezvareh station. This may be related to the non significant differences among erosivity data for different seasons. Also, significantly differences in seasonal erosivity for different stations verified the importance of considering seasonality for erosivity calculations.Based on regression method, seasonal regression models showed adjusted R^2 and E values ranging from 0.62 to 0.87 and E1 ranging from 0.38 to 0.64 (Table 4). Six regional regression models were created to predict erosivity from rainfall in spring, summer, autumn, winter, dry and wet seasons (Table 4 and Fig. 2).

An analysis of the 25 highest values in maximum 30-min rainfall intensity for each station showed that 65 % of these events occurred during the wet seasons. Predicted seasonal erosivity data have showed that autumn and summer season have highest values. Sadeghi and Behzadfar, (2005) reported similar results from a study in adjacent province of the study area (Mazandaran). Considering cropping pattern, in this period, agricultural area have low ground canopy and cover because in this region cropping season was started in mid of autumn and was stopped in beginning of summer (Kelarestaghi *et al.,* 2009). So, it is necessary to compile crop management program (Mikhailova *et al.,* 1997) and rotation strategies (Laflen and Moldenhauer, 2003). All cropland areas in north of Iran have similar conditions.

Erosivity showed differences among wet and dry seasons. The regression model of the wet seasons had a higher slope than the dry seasons. So, there was a higher increase in erosivity during the wet seasons, for every unit increase in rainfall amount. The results showed that summer season with having lower frequency of rainfall event (n = 191) than other seasons (autumn = 371, winter = 348 and spring = 280) had higher mean erosivity (144.2 MJ/mm/ ha/ hr) than other seasons (autumn = 82.8, winter = 59.56 and spring = 78.2 MJ /mm /ha/ hr). These results indicate importance of a higher frequency of large and intense storms during summer season.

In addition, the results showed mean annual erosivity in the study area is 8408.58 MJ/mm /ha/ hr. Minimum and maximum amounts of erosivity were calculated in June and November, respectively. This condition is resulted from decrease and increase of rainfall amount. Findings is in accordance with the results from Alexandre, (2004) in Brazil, Hoyos *et al.,* (2005) in Colombia, Davison *et al.,* (2005) in England and Wales, and Shamshad *et al.,* (2008) in Malaysia.

Despite the general spatial pattern, differences were evident between the models. With comparing two interpolation methods, the local polynomial method was selected because of lower mean prediction error and comparable root mean square prediction errors (Table 5). Hoyos *et al.,* (2005) also, found better results

Table 1. Characteristics of the study area rain gauge stations

Rain gauge stations	Latitude northing	Longitude easting	Elevation (m)	Length of records (years)	Average annual rainfall (mm)	Average annual erosive rainfall (>12.7) (mm)	Years with missing data
Agh Ghala [P.G]	37° 01′	54° 28′	-12	12	429.11	252.6	0
Ghafarhaji [P.G]	37° 00′	54° 08′	-33	12	546	294.49	0
Fazal Abad [P.G]	36° 54′	54° 45′	210	12	699.75	406.2	0
Lezvareh [P.G]	37° 14′	55° 22′	155	12	882.66	597.4	0
Park –e- Melli [P.G]	37° 16′	55° 55′	460	8	1007.32	686.66	4
Golidagh [P.G]	37° 39′	56° 00′	1000	7	819.34	497.29	5
Sad –e- Gorgan [P.M]	37° 12′	54° 44′	12	12	346.34	-	0
Gonbad [P.M]	37° 15′	55° 10′	37	12	456.95	-	0
Tamar [P.M]	37° 29′	55° 30′	132	12	574.92	-	0
Nodeh [P.M]	37° 04′	55° 16′	280	12	926.29	-	0
Zaringol [P.M]	36° 52′	54° 57′	280	12	874.56	-	0
Gharnagh [P.M]	37° 43′	55° 43′	500	9	455.21	-	3
Til Abad [P.M]	36° 55′	55° 28′	1000	12	224.38	-	0
Cheshmeh Khan [P.M]	37° 18′	56° 07′	1250	12	215.75	-	0
Rabat Gharebil [P.M]	37° 21′	56° 19′	1295	12	186.36	-	0
Shirin Abad [P.M]	36° 47′	55° 01′	882	9	602.28	-	3
Khosh Yeilagh [P.M]	36° 85′	55° 35′	1740	6	421.24	-	6

[P.G]. Pluviographic data used to calculate the EI_{30} index
[P.M]. Pluviometric data (monthly totals) used to model regional erosivity

Table 2. The results of regression model and evaluation of model performance for storm EI_{30} (log MJ mm^{-1} ha^{-1} h^{-1}) versus storm rain (log mm) in pluviograph stations

Rain gauge stations	n	Intercept	Slope	RMSE	R^2	E	E_1
Agh Ghala	53	-0.336	1.51	0.40	0.22 **	0.22	0.12
Ghafarhaji	89	-0.745	1.74	0.34	0.46 **	0.46	0.27
Fazal Abad	129	-0.757	1.81	0.39	0.39 **	0.40	0.21
Lezvareh	54	-1.191	1.99	0.37	0.50 **	0.50	0.27
Park –e- Melli	66	-1.393	2.07	0.38	0.51 **	0.51	0.29
Golidagh	29	-0.92	1.75	0.36	0.51 **	0.51	0.28

** Significance in level of 99%

Table 3. The results of seasonal EI_{30} and their statistical comparisons for pluviographic stations

Rain gauge stations	n	Seasonal EI_{30} values (MJ mm ha^{-1} season^{-1})			
		Autumn	Winter	Spring	Summer
Agh Ghala	42	355.9 c	181.7 a	213.2 ab	285.7 b
Ghafarhaji	42	475.5 c	118.8 a	102.3 a	275.5 b
Fazal Abad	48	496.5 bc	243.1 a	393.3 b	300.2 ab
Lezvareh	48	455.4 a	415.3 a	308.7 a	425.2 a
Park –e- Melli	48	481.9 a	484.5 a	574.3 a	814.3 b
Golidagh	45	334.2 ab	293.7 a	282.9 a	460.0 b
Mean	273	433.23 b	289.52 a	312.45 a	426.82 b

Values showed by different letters within the same line are significantly different from each other (α=0.05, Tukey-Kramer test)

Table 4. The results of regression model and evaluation of model performance for seasonal EI_{30} (log MJ mm^{-1} ha^{-1} h^{-1} season^{-1}) versus seasonal rain (log mm) in pluviograph stations and in regional scale

	Stations	n	Intercept	Slope	RMSE	R^2	E	E_1
Rain gauge stations	Agh Ghala	42	0.379	1.07	0.22	0.66 **	0.67	0.51
	Ghafarhaji	42	0.138	1.12	0.25	0.62 **	0.63	0.38
	Fazal Abad	48	0.011	1.23	0.21	0.70 **	0.71	0.48
	Lezvareh	48	0.242	1.07	0.10	0.86 **	0.87	0.64
	Park –e- Melli	48	-0.31	1.37	0.17	0.84 **	0.84	0.55
	Golidagh	45	-0.028	1.24	0.22	0.76 **	0.76	0.52
Regional scale	Autumn	71	0.19	1.13	0.17	0.76 **	0.77	0.57
	Winter	71	0.218	1.28	0.2	0.81 **	0.81	0.58
	Spring	69	0.322	1.05	0.25	0.66 **	0.67	0.45
	Summer	62	0.333	1/12	0.17	0.79 **	0.8	0.52
	Wet season	142	-0.099	1.24	0.19	0.79 **	0.79	0.56
	Dry season	131	0.326	1.09	0.22	0.70 **	0.76	0.49

** Significance in level of 99%

Table 5. The results for comparison of different interpolation methods in producing isoerodent maps

Season	Methods	Power	Prediction errors (MJ mm ha^{-1} h^{-1} season^{-1})	
			Mean	RMSE
Autumn	Inverse distance weighted	2	71.84	235.60
	Local polynomial	1	-32.68	177.20
Winter	Inverse distance weighted	2	61.11	191.44
	Local polynomial	1	-27.92	144.80
Spring	Inverse distance weighted	2	105.61	253.48
	Local polynomial	1	-14.52	183.40
Summer	Inverse distance weighted	2	94.32	254.64
	Local polynomial	1	-38.02	193.70
Wet	Inverse distance weighted	2	142.83	433.71
	Local polynomial	1	-60.30	314.40
Dry	Inverse distance weighted	2	222.64	551.17
	Local polynomial	1	-64.04	405.20

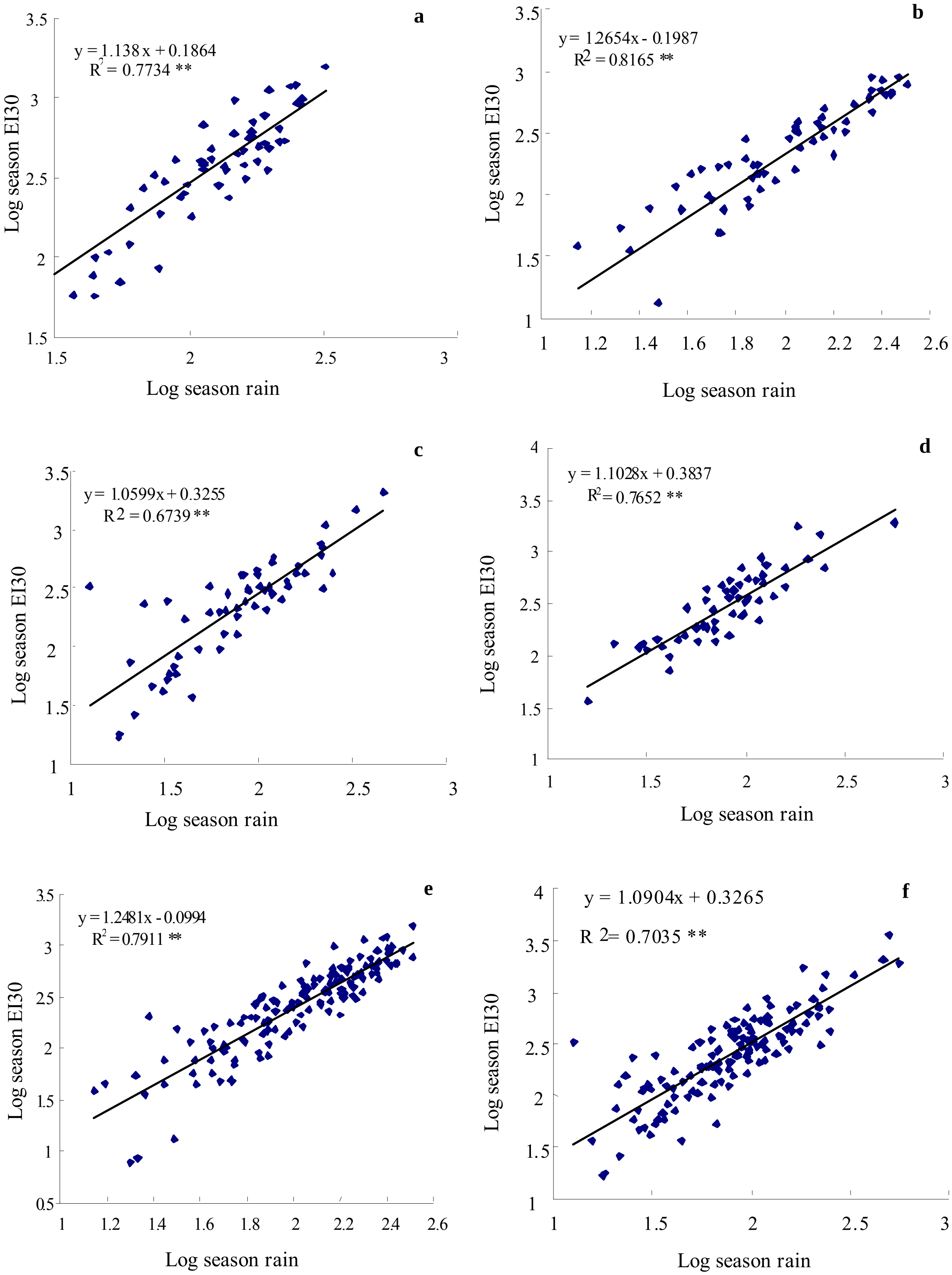

Fig. 2. Regional-seasonal erosivity models for the (a) autumn, (b) winter, (c) spring, (d) summer, (e) wet and (f) dry seasons of seasonal EI_{30} (MJ mm ha^{-1} h^{-1} season^{-1}) and rain (mm), using all pluviographic records

when applied local polynomial algorithm than the IDW in the Colombian Andes. The interpolation of erosivity values from 17 rainfall stations (6 pluviographic and 11 pluviometric stations) resulted in 6 isoerodent surfaces, four for each season, one for the wet seasons and one for the dry seasons (Fig. 3). Variability in all 6 isoerodent surfaces indicates a similar pattern, approximately. In all cases, the highest values of erosivity were at the middle parts of the study area and lowest to eastern and western parts of the study area. The erosivity gradient was steeper in the wet season than in the dry season.

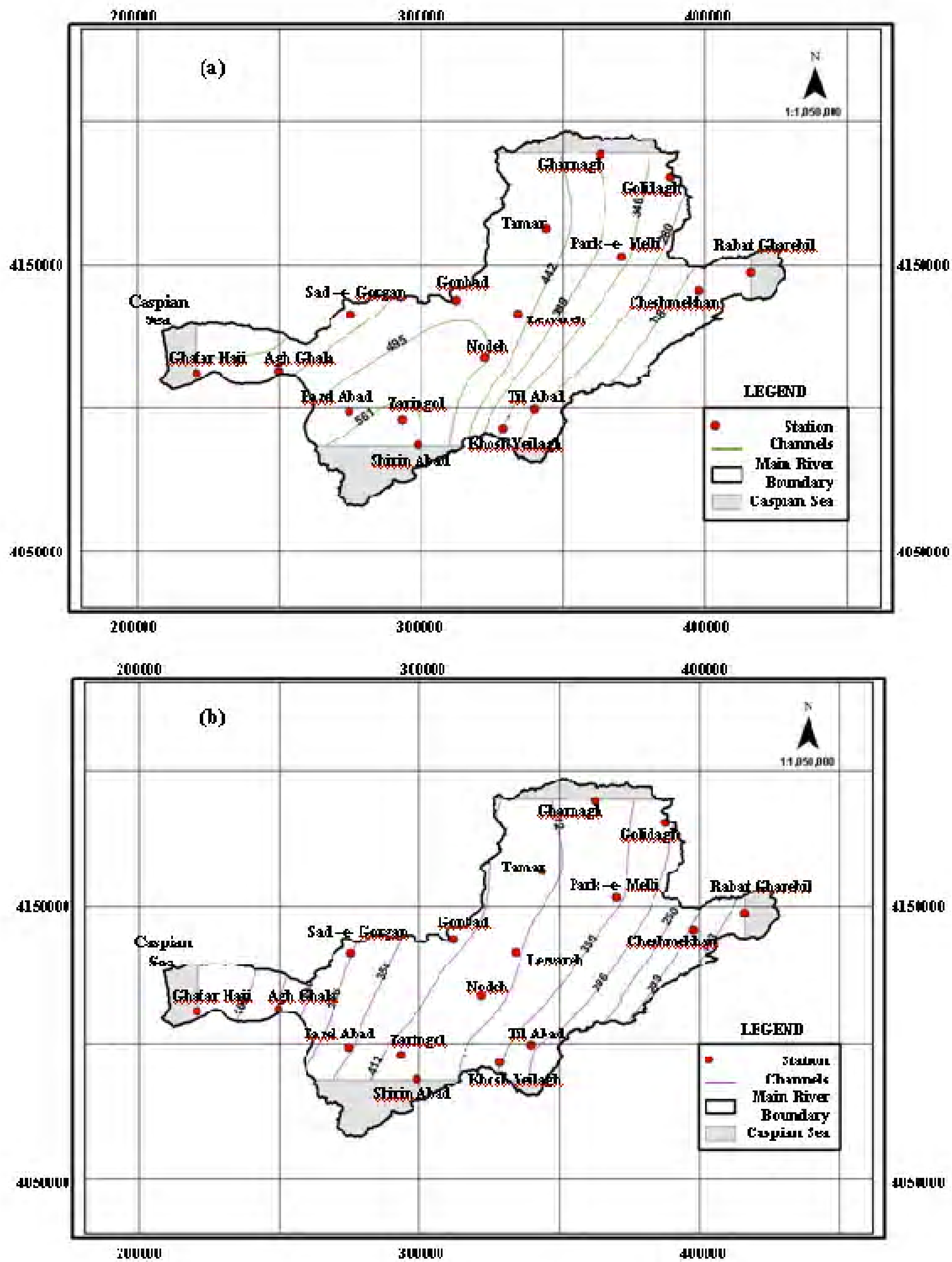

Fig. 3. Isoerodent maps for the (a) autumn, (b) winter, (c) spring, (d) summer, (e) wet and (f) dry seasons using all pluviographic and pluviometric data (Continues)

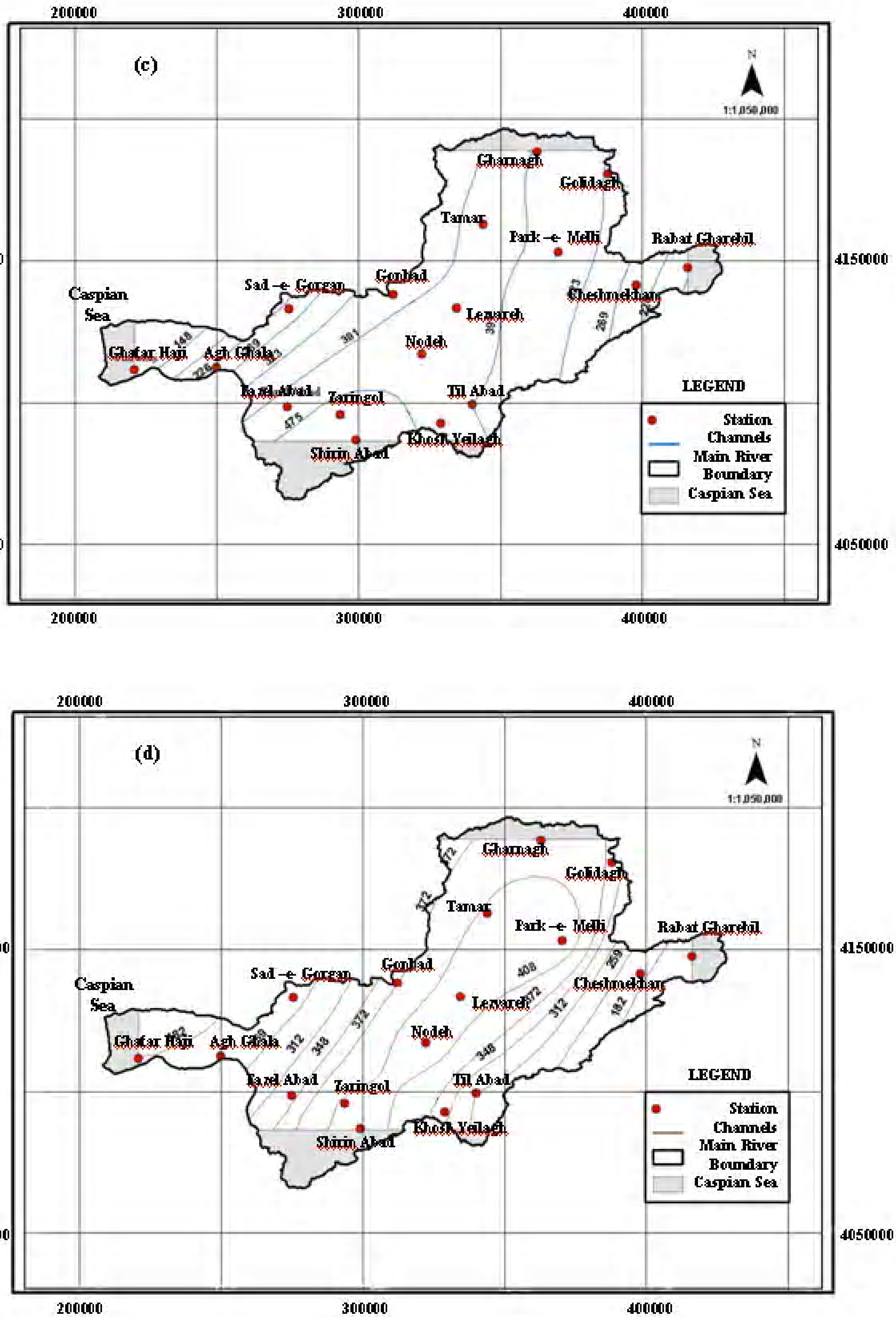

Fig. 3. Isoerodent maps for the (a) autumn, (b) winter, (c) spring, (d) summer, (e) wet and (f) dry seasons using all pluviographic and pluviometric data (Continues)

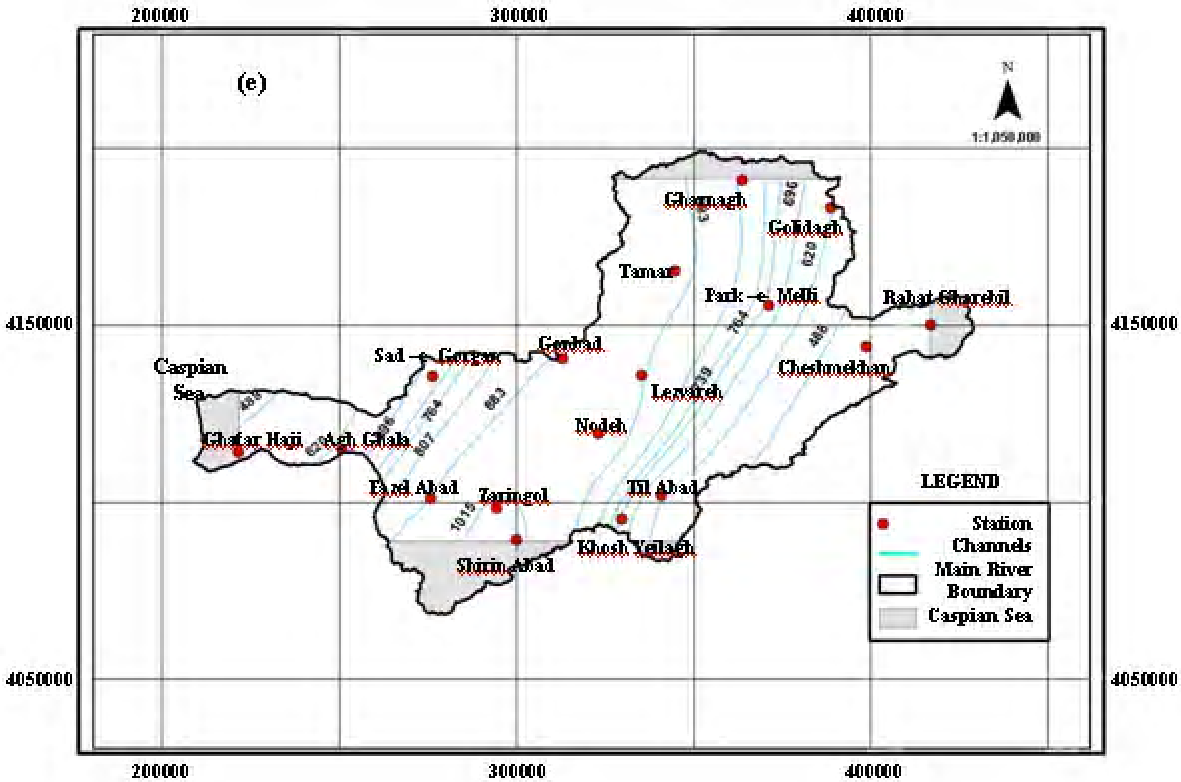

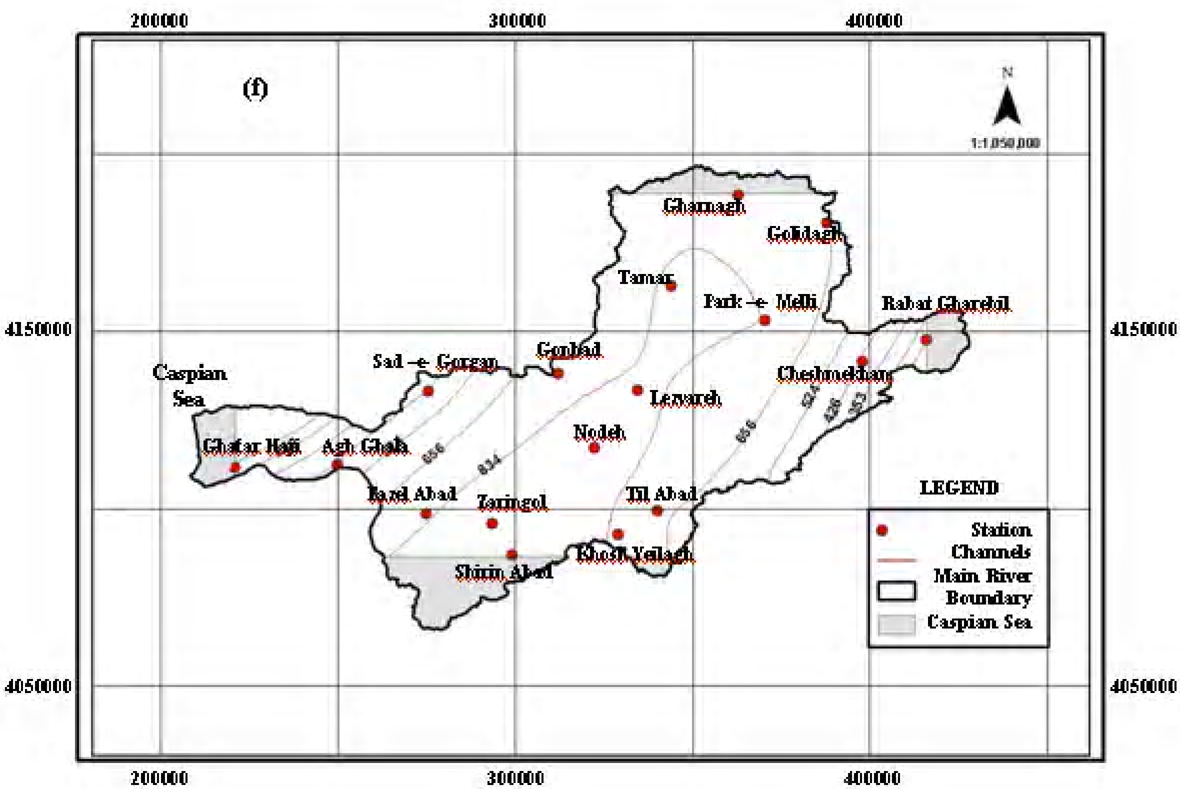

Fig. 3. Isoerodent maps for the (a) autumn, (b) winter, (c) spring, (d) summer, (e) wet and (f) dry seasons using all pluviographic and pluviometric data (Continue)

During the wet season, erosivity varied from 438 Mj/mm/ha (west) to 1015 Mj/mm/ha (Middle). But, in the dry season, values of erosivity were lower than from values in wet season and the highest values were at the middle parts of the study area and the lowest were at the eastern and the western parts of the study area (Fig 3). This pattern is similar to the distribution of the extreme rainfall events in the region and is an indicator of the EI_{30} index being closely related to the most intense rainfall events. These variations were compared with elevations, longitude, latitude and distance to humid source to analyze spatial pattern. Results showed similar relationships between these parameters and annual erosivity in pluviograph stations (except Golidagh station).

The Findings, also, indicate high variability in the spatial patterns of rainfall erosivity within relatively short distances. For example, during the dry season, observed erosivity at Park -e- Melli station was 87% higher than at Golidagh station (1388.6 vs. 742.9 MJ/ mm/ ha/season), although above mentioned stations were only 40 km apart. This percentage during the wet season was 54% (966.4 vs. 627.9 MJ/mm/ ha/season). Many parameters such as elevation, local topography, longitude, latitude and distance to humid source may be affecting on variability of erosivity.

Generally the results showed that the annual erosivity in this area increases with elevation up to 460 m (Park -e- Melli) and then decreases. So, the effect of elevation on rainfall amount depicts increasing in erosivity values from northeast and northwest to south. Millward and Mersey, (1999) reported that erosivity and precipitation increased with elevation. Whereas, Mikhailova *et al.*, (1997) found that in Costa Rica, Seri Lanka and southern US, there was an inverse relation between erosivity and elevation. The results, also, showed annual rainfall and consequently annual erosivity decreases up to Golidagh station with increasing in latitude. In the case of distance to humid source, the findings of this study indicated that there are an inverse relation between distance to humid source (Caspian Sea in western parts of the study area) and erosivity values. According to priority, the highest erosivity risk observed in Park -e- Melli station. Aside Golidagh station, rainfall erosivity increases from west to east. Sadeghi and Behzadfar, (2005) reported increasing erosivity from west to east in Mazandaran province where is located in adjacent of the study area.

CONCLUSION

In conclusion, we analyzed 420 intensity data based on 13 years of records of 6 pluviograph stations in northeast of Iran and developed regression relationships between storm rain and EI_{30} in regional scale. Then, by integrating 11 pluviometric monthly data, we developed six seasonal-regional rainfall erosivity models. Our findings provide a good guidance to integrate pluviograph and pluviometric data for rainfall erosivity assessment in regional scales, where short duration rainfall intensity data, usually are not available.

The results of this study also, can be helpful in the application of soil erosion prediction models such as USLE and RUSLE and soil conservation programs in Golestan province (study area) where suffered many floods in years 2001 to 2003 and many volumes of sediment delivered to two downstream dams. For future, it is necessary to develop better surfaces of seasonal-regional erosivity with respect to the year to year as well as within- year variations improvement.

ACKNOWLEDGEMENT

The authors would like to thank Sari Agricultural Sciences and Natural Resources University (SANRU) for the funding of project. We also thank to regional water organization of Golestan province for data supporting and to two anonymous reviewers for constructive comments.

REFERENCES

Abu Hammad, A., Lundekvam, H. and Borresse, T. (2004). Adaptation of RUSLE in the Eastern Part of the Mediterranean Region. Environmental Management, **34 (6)**, 829-841.

Alexandre, M. D. S. (2004). Rainfall erosivity map for Brazil. Catena, **57**, 251- 256.

Angulo-Martýnez, M., Lopez-Vicente, M., Vicente-Serrano, S. M. and Beguera, S. (2009). Mapping rainfall erosivity at a regional scale: a comparison of interpolation methods in the Ebro Basin (NE Spain). Hydrology and Earth System Sciences Discussions, **6**, 417-453.

Davison, P., Hutchins, M. G., Anthony, S. G., Betson, M., Johnson, C. and Lord, E. I. (2005). The relationship between potentially erosive storm energy and daily rainfall quantity in England and Wales. Science of the total Environment, **344**, 15- 25.

Foster, G. R. (2004). User's Reference Guide. Revised Universal Soil Loss Equation, Version2. National Sedimentation Laboratory, USDA–Agricultural Research Service Oxford, Mississippi.

Gonzalez-Hidalgo, J. C., Pena-Monne, J. L. and de Luis, M. (2007). A review of daily soil erosion in western Mediterranean areas. Catena, **71**, 193–199.

Goovaerts, P. (1999). Using elevation to aid the geostatistical mapping of rainfall erosivity. Catena, **34**, 227–242.

Hoyos, N., Waylen, P. R. and Jaramillo, A. (2005). Seasonal and spatial patterns of erosivity in a tropical watershed of the Colombian Andes. Journal of Hydrology, **314**, 177-191.

Johnston, K., Ver Hoef, J. M., Krivoruchko, K. and Lucas, N. (2001). Using ArcGIS Geostatistical Analyst. ESRI Press, Redlands.

Julie, P. (2001). A step by step guide to data analysis using SPSS for windows. Open University Press.

Kelarestaghi, A., Ahmadi, H., Esmali Ouri, A., Jafari, M. and Ghodosi, J. (2009). Comparison of runoff and sediment yield from different agricultural treatments. Journal of Iran-Watershed Management Science & Technology, **5**, 41-52 (in Persian).

Laflen, J. M. and Moldenhauer, W. C. (2003). Pioneering soil erosion prediction- The USLE story, World Association of Soil & Water Conservation (WASWC), Special Publication No. 1, 54 pp.

Lal, R. (1990). Soil Erosion in the tropics: Principles and Management. Mc Graw– Hill, New York.

Lal, R. (1998). Drop size distribution and energy load of rain storms at Ibadan, western Nigeria. Soil & Tillage Research, **48**, 103-114.

Legates, D. R. and Mc cable, G. J. (1999). Evaluating the use of goodness of – fit measures in hydrologic and hydroclimatic model validation. Water Resources Research, **35**, 233–241.

Lim, K. J., Sagong, M., Engel, B. A., Tang, Z., Choi, J. and Kim, K. (2005). GIS-based sediment assessment tool. Catena, **64**, 61-80.

Men, M., Yu, Z. and Xu, H. (2008). Study on the spatial pattern of rainfall erosivity based on geostatistics in Hebei province, China. Frontiers of Agriculture in China, **2 (3)**, 281-289.

Mikhailova, E. A., Bryant, R. B., Schwager, S. J. and Smith, S. D. (1997). Predicting rainfall erosivity in Honduras. Soil Science Society of America journal, **61**, 273-279.

Millward, A. A. and Mersey, J. E. (1999). Adapting the RUSLE to model soil erosion potential in a mountainous tropical watershed. Catena, **38**, 109-129.

Mutua, B. M., Klik, A. and Loiskandl, W. (2006). Modeling soil erosion and sediment yield at a catchment scale: the case of masinga catchment, Kenya. Land Degradation & Development, **17**, 557–570.

Nash, J. E, and Sutcliffe, J. V. (1970). Rive flow forecasting through conceptual models. I. A discussion of principles. Journal of Hydrology, **10**, 282-290.

Renard, K. G. and Freimund, R. (1994). Using monthly precipitation data to estimate the R–factor in the revised USLE. Journal of Hydrology, **157**, 287-306.

Renard, K. G., Foster, G. R., Weesies, G. A., Mc Cool, D. K., and Yoder, D. C. (1997). Predicting soil erosion by water: a guide to conservation planning with the revised universal soil loss equation (RUSLE). USDA Handbook 703, Washington, DC.

Sadeghi, S. H. R. and Behzadfar, M. (2005). Spatial variation of rainfall erosivity in Mazandaran province, Iran. Pajoheshnameh Khazar, **3 (1)**, 36-47 (in Persian).

Shamshad, A., Azhari, M. N., Isa, M. H., Wan Hussin, W. M. A. and Parida, B. P. (2008). Development of an appropriate procedure for estimation of RUSLE EI_{30} index and preparation of erosivity maps for Pulau Penang in Peninsular Malaysia. Catena, **72**, 423-432.

Shi, Z. H., Cai, C. F., Ding, S. W., Wang, T. W. and Chow, T. L. (2004). Soil conservation planning at the small watershed level using RUSLE with GIS. Catena, **55**, 33–48.

Thomann, R. V. (1982). Verification of water quality models. Journal of Environmental Engineering Division, **108 (5)**, 923–940.

Warner, G. S., Stake, J. D., Guillard, K. and Neafsey, J. (1997). Evaluation of EPIC for a shallow New England soil: II. Soil nitrate. Transactions of the ASAE, **40 (3)**, 585–593.

Winchell, M. F., Jackson, S. H., Wadley, A. M. and Srinivasan, R. (2008). Extension and validation of a geographic information system-based method for calculating the Revised Universal Soil Loss Equation length-slope factor for erosion risk assessments in large watersheds. Journal of Soil and Water Conservation, **63**, 105–111.

Wischmeier, W. H. and Smith, D. D. (1978). Predicting fainfall erosion losses: a guide to conservation planning .USDA Handbook 537, Washington, DC.

Yu, B. (1998). Rainfall erosivity and its estimation for Australia's Tropics, Australian. Journal of Soil Research, **36**, 143-165.

Yu, B., Hashim, G. M. and Eusof, Z. (2001). Estimating the R–factor with limited rainfall data: a case study from Peninsular Malaysia. Journal of soil and water conservation, **6**, 101–105.